

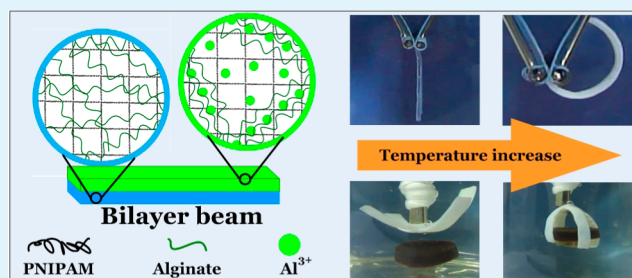
Tough Al-alginate/Poly(*N*-isopropylacrylamide) Hydrogel with Tunable LCST for Soft Robotics

Wen Jiang Zheng,[†] Ning An,[‡] Jian Hai Yang,[†] Jinxiong Zhou,^{*,‡} and Yong Mei Chen^{*,†}

[†]School of Science, State Key Laboratory for Mechanical Behaviour of Materials, Collaborative Innovation Center of Suzhou Nano Science and Technology, and [‡]State Key Laboratory for Strength and Vibration of Mechanical Structures and School of Aerospace, Xian Jiaotong University, Xi'an 710049, P. R. China

ABSTRACT: Tough Al-alginate/poly(*N*-isopropylacrylamide) (PNIPAM) hydrogel has been synthesized by introducing an interpenetrating network with hybrid physically cross-linked alginate and chemically cross-linked PNIPAM. Varying the concentration of AlCl₃ regulates the mechanical properties of the tough hydrogel and tunes its lower critical solution temperature (LCST) as well. The tough Al-alginate/PNIPAM exhibits 6.3 ± 0.3 MPa of compressive stress and 9.95 of uniaxial stretch. Tunability of LCST is also achieved in a wide range within 22.5–32 °C. A bending beam actuator and a four-arm gripper made of bilayer (Na-alginate/PNIPAM)/(Al-alginate/PNIPAM) hydrogel as prototype of all-hydrogel soft robotics are demonstrated. A finite element (FE) simulation model is developed to simulate the deformation of the soft robotics. The FE simulation not only reproduces the deformation process of performed experiments but also predicts more complicated devices that can be explored in the future. This work broadens the application of temperature-responsive PNIPAM-based hydrogels.

KEYWORDS: hydrogels, tough, LCST, actuator, robotics



1. INTRODUCTION

Stimuli-response hydrogels have found tremendous applications as adaptive lenses,^{1,2} artificial muscles,^{3,4} vehicles for drug deliveries,^{5,6} scaffolds or matrices for tissue engineering,^{7,8} as well as sensors and actuators for soft robotics and soft machines.^{9,10} As a typical stimulus-responsive hydrogel, poly(*N*-isopropylacrylamide) (PNIPAM) has been extensively explored for various applications,^{11–14} largely due to the fact that temperature is readily to be manipulated. Traditional PNIPAM hydrogels are fragile with low strength ~5 kPa¹⁵ and modulus ~10 kPa.¹⁴ The applications of PNIPAM-based hydrogels, thus far, are limited mainly to the cases where stress level is rather low, e.g., drug delivery carriers,^{5,6} cell culture scaffolds,^{7,8} actuator in biological applications, etc. Enhancing the mechanical performance will extend the application area of hydrogels to soft machine. Several toughening mechanisms have been proposed to enhance the mechanical properties of PNIPAM-based hydrogels. Cross-linking by covalent bonds, PNIPAM-based double-network hydrogel achieves strengths of ~17.5 MPa in compression;¹⁶ cross-linking by clay nanosheets through hydrogen bonds, nanocomposite PNIPAM hydrogel attains ~1 MPa of tensile strength;¹⁷ cross-linking by nanogels through covalent bonds, nanostructured PNIPAM hydrogel shows tensile strength ~240 kPa.¹⁸

The most appealing feature of PNIPAM-based hydrogels is their volume phase transition across the lower critical solution temperature (LCST). The above-mentioned mechanical enhanced PNIPAM-based hydrogels exhibit a fixed LCST,

approximately 32 °C. Reducing the LCST enables operation of PNIPAM-based hydrogel devices at lower temperature, such as ambient temperature, and avoids the complexity of additional heating to trigger the onset of phase transition. This will extend the application of PNIPAM-based hydrogels to actuators, robotics, self-folding structures, and pattern formation.^{19–21}

Very few efforts, to our best knowledge, have been conducted to synthesize tough PNIPAM-based hydrogels with tunable LCST and utilize them as hydrogel actuator. In this contribution, we describe a facile approach to synthesize tough Al-alginate/PNIPAM hydrogels with tunable LCST. Interpenetrating of long-chain networks by reversible ionically cross-linked alginate and chemically cross-linked PNIPAM is inspired by previous tough alginate/polyacrylamide (PAAm) hydrogels.^{22,23} Mechanical strength and Young's modulus of the Al-alginate/PNIPAM hydrogel show 1 order of magnitude of increase as compared with pure PNIPAM or Na-alginate/PNIPAM hydrogels. Interestingly, modulating the AlCl₃ concentration can tune the LCST of Al-alginate/PNIPAM hydrogels to a wide range within 22.5–32 °C. We design and fabricate a bilayer cantilever beam and a four-arm gripper structure made of (Na-alginate/PNIPAM)/(Al-alginate/PNIPAM) hydrogel as proof-of-concept demonstrations of all-hydrogel soft robotics. The bending angle of bilayer cantilever beam reaches as large as ~140° at 30

Received: October 23, 2014

Accepted: January 5, 2015

Published: January 5, 2015

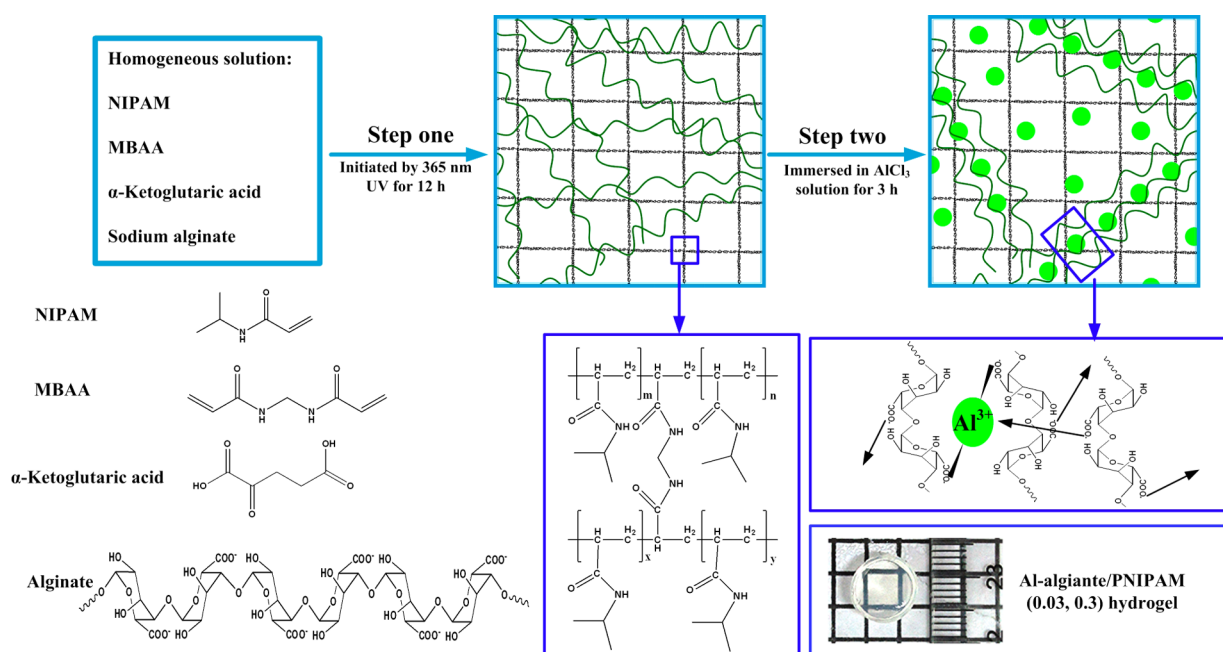


Figure 1. Two-step method to synthesize Al-alginate/PNIPAM hydrogels. In step one, the NIPAM monomers are polymerized and cross-linked through chemical bonding. In step two, the alginate polymers are physically cross-linked through the electrostatic interaction between the Al^{3+} cations and carboxylate groups (COO^-), resulting a transparent tough hydrogel. Mobile AlCl_3 cations prevail in the hydrogel network as a small piece of hydrogel sample is immersed in a bulk AlCl_3 solution.

$^{\circ}\text{C}$ with respect to $\sim 90^{\circ}$ in previous report,¹² and the four-arm gripper fulfills a grasping action under water. Finite element (FE) simulation based on the deswelling kinetics of those hydrogels is also performed to study the all-hydrogel bilayer beam and the four-arm gripper, which is helpful for understanding and controlling the motions of the soft robotics. The results of experiment fit the simulation very well.

2. EXPERIMENTAL SECTION

2.1. Regent and Materials. *N*-Isopropylacrylamide (NIPAM, 99%) as the monomer, *N,N'*-methylenebis(acrylamide) (MBAA, 99%) as the chemical cross-linker, and α -ketoglutaric acid (98%) as the initiator were purchased from Sigma-Aldrich. Sodium alginate (AR) and aluminum chloride (AR) as physical cross-linker were purchased from Aladdin.

2.2. Hydrogels Synthesis. Al-alginate/PNIPAM hydrogels were prepared by a two-step method. In the first step, NIPAM, alginate powder, α -ketoglutaric acid, and MBAA were dissolved in deionized water to obtain a homogeneous solution. The solution was transferred into a mold and irradiated by the UV light (wavelength of 365 nm) for 12 h and resulted in the Na-alginate/PNIPAM hydrogel. In the second step, the Na-alginate/PNIPAM hydrogel was immersed in an aqueous solution containing AlCl_3 for 3 h, and the diffused Al^{3+} ions cross-linked alginate polymers and ultimately obtained the Al-alginate/PNIPAM hydrogel. The performance of Al-alginate/PNIPAM (x, y) hydrogels can be tuned by changing the concentration of MBAA (x is the MBAA concentration in mol % with respect to NIPAM monomer, $x = 0.01, 0.03, 0.05, \text{ and } 0.07$ mol %) and Al^{3+} (y is Al^{3+} concentration, $y = 0.1, 0.3, 0.5, \text{ and } 0.7$ mol/L). Pure PNIPAM hydrogel was prepared by UV irradiation of the solution of NIPAM, α -ketoglutaric acid, and MBAA for 12 h.

2.3. Mechanical Properties Test. The tensile and compressive experiments were performed using a tensile-compressive tester (CMT6503, MTS, U.S.A.). The samples for tensile tests were cut into a dumbbell shape, and the size of tensile part was $12 \times 2 \times 2$ mm. Testing was performed at the speed of 100 mm/min. The modulus of hydrogel samples was obtained by calculating the slope of the stress–stretch curve at stretch 0–1.0. The critical tensile strength was measured at the

fractured point. For compressive test, the samples were cut into a disk shape with radius of 8 mm and thickness of 5–6 mm and compressed at a strain rate of $10\% \text{ min}^{-1}$. Both tensile and compressive tests were performed at temperature around 20°C . The Young's modulus and failure strength for compressive tests are determined as that for tensile tests.

2.4. Thermoresponsive Property Test. Water uptake of hydrogels as a function of temperature was studied gravimetrically. Each hydrogel sample was put into a beaker and immersed in deionized water. The temperature was controlled by a water bath pot. The samples were taken out of the beaker, and the surface water was removed by filter paper to measure the sample mass (W_T) when a prescribed temperature ($T^{\circ}\text{C}$) was reached. Then the samples were kept in a baking oven for 48 h at 50°C , and the weights (W_d) of the corresponding dried gels were measured. The temperature dependent water uptake (W) was calculated using eq 1.

$$W = (W_T - W_d) / W_d \quad (1)$$

The LCST was defined as the temperature when W of hydrogels began to decline.

The eq 2 is used for calculating the water uptake (M) in the deswelling process of hydrogels at a set temperature. In this case, the samples were transferred from a 20°C water bath to a 45°C one. The time dependence gel weight (M_t) of each sample was measured when a prescribed immersing time (t_s) was reached in 45°C water bath. In each measurement, the gel was taken out from the 45°C water bath and removed the surface water by filter paper and weighted. The whole measurement process for each sample was carried out within 10 s. Then the samples were kept in an oven for 48 h at 50°C , and the weights (M_d) of the corresponding dried gels were measured.

$$M = (M_t - M_d) / M_d \quad (2)$$

2.5. Preparation of Soft Robotics. The bilayer hydrogel beam was prepared by two steps. First, the Al-alginate/PNIPAM (0.03, 0.7) was prepared as the method mentioned above. Then one piece of transparent Al-alginate/PNIPAM (0.03, 0.7) hydrogel and one piece of glass are used as the mold to synthesize the bilayer hydrogel. The solution containing NIPAM, alginate, MBAA, and α -ketoglutaric acid was poured into the mold and irradiated by the UV light (wavelength of

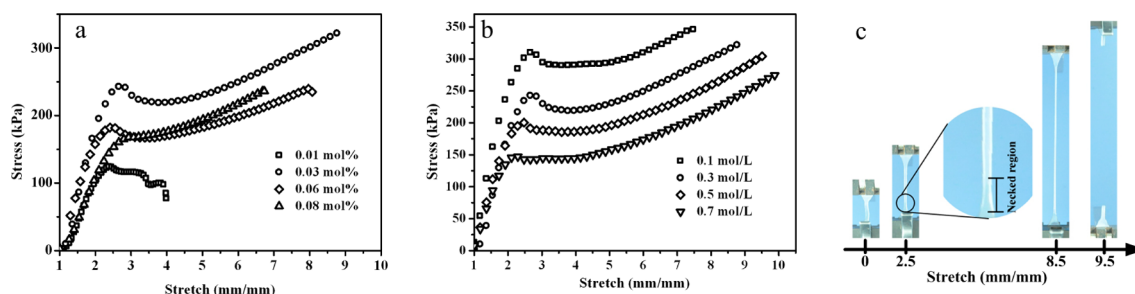


Figure 2. Tensile test of the Al-alginate/PNIPAM hydrogels. (a) Stress–stretch curves of Al-alginate/PNIPAM ($x, 0.3$) hydrogel, x is the concentration of MBAA, $x = 0.01, 0.03, 0.06, 0.08$ mol %; (b) stress–stretch curve of Al-alginate/PNIPAM ($0.03, y$) hydrogel, y is the concentration of Al^{3+} , $y = 0.1, 0.3, 0.5, 0.7$ mol/L; (c) images of the Al-alginate/PNIPAM ($0.03, 0.3$) hydrogel in the tensile test at different stretch; a necked region appeared at stretch of 2.5 which reflects a yield point in the stress–stretch curves.

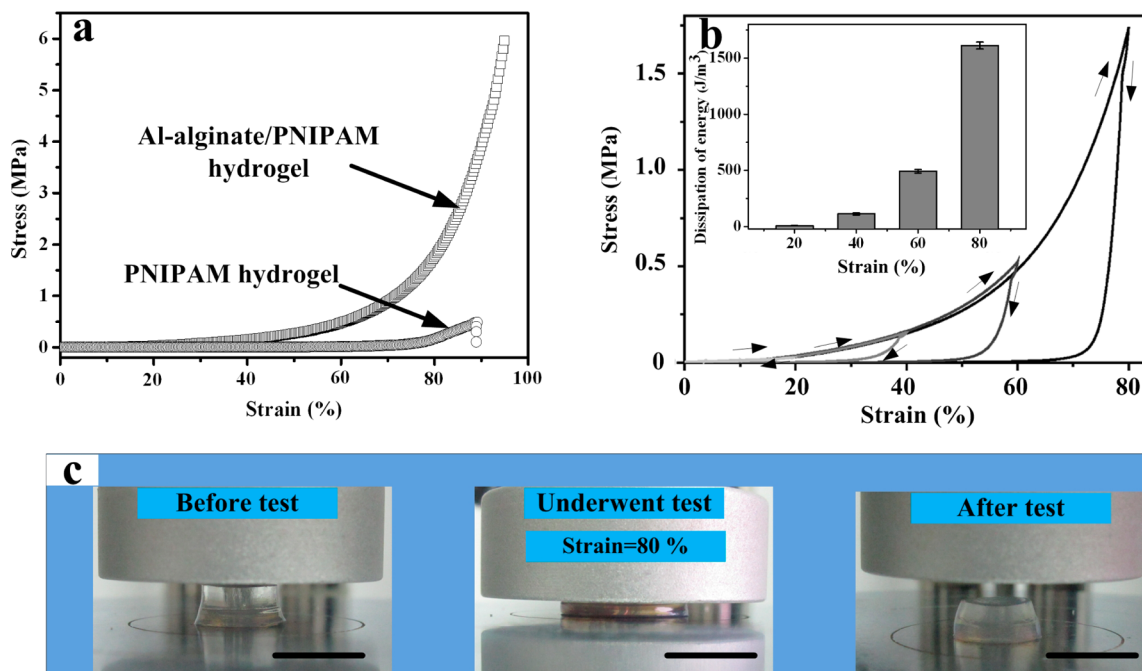


Figure 3. Compressive test of the tough Al-alginate/PNIPAM ($0.03, 0.3$) hydrogel. (a) Stress–strain curves of the tough hydrogel and PNIPAM hydrogel for comparison. (b) Loading and unloading curves with insertion of dissipated energy per complete cycle. (c) Images of the tough hydrogel before, compressed 80%, and after the compression, respectively. The scale bar is 10 mm.

365 nm) for 12 h, the bilayer (Na-alginate/PNIPAM)/(Al-alginate/PNIPAM) was obtained, and the Na-alginate/PNIPAM hydrogel was directly grown on the surface of Al-alginate/PNIPAM hydrogel. The gripper was designed by crossing two pieces of bilayer hydrogel beam as an X-shape.

3. RESULTS AND DISCUSSION

We synthesize Al-alginate/PNIPAM hydrogel using the two-step method schematized in Figure 1. In the first step, PNIPAM was loosely chemically cross-linked by N,N' -methylenebis(acrylamide) (MBAA), while uncross-linked Na-alginate linear polymers were well-dispersed in the PNIPAM long-chain networks, resulting in Na-alginate/PNIPAM hydrogel. Then in the second step, the Na-alginate/PNIPAM hydrogel was immersed in a AlCl_3 solution for 3 h, allowing diffusion of Al^{3+} cations in the polymer networks and exchange of Na^+ ions by Al^{3+} ions ($3\text{Na}^+ \rightarrow \text{Al}^{3+}$). Thus, Na-alginate can be cross-linked by stable Al-carboxylate coordination bond between Al^{3+} ions and carboxylate groups ($\text{Al}(\text{COO})_3$), and transparent tough Al-alginate/PAAm hydrogel (x, y) was obtained, where x is the MBAA concentration in mol % with respect to NIPAM

monomer and y is the Al^{3+} concentration. The trivalent Al^{3+} ions cross-link alginate polymers in two different planes at the same time, forming a compact 3D valent bonding structure with the alginate.^{23,24} Excessive mobile AlCl_3 also prevails in the hydrogel networks.

The concentration of MBAA is continuously varied to achieve optimal synthesis conditions. Figure 2a presents the uniaxial tensile test results of Al-alginate/PNIPAM ($x, 0.3$) hydrogels, where x is the MBAA concentration in mol % with respect to NIPAM monomer ($x = 0.01, 0.03, 0.06, 0.08$ mol %), and Al^{3+} concentration is 0.3 mol/L. The MBAA concentration affects the critical stretches obviously, and the tough Al-alginate/PNIPAM ($0.03, 0.3$) hydrogel exhibits the highest tensile stress of 322 ± 9.1 kPa, Young's modulus of 185 ± 18.3 kPa, and ~ 9 of uniaxial stretch. This is understood as follows. When the cross-linking concentration of MBAA is too low, the hydrogel networks become too compliant and unable to sustain stress. In the other extreme, the cross-linking concentration is too high, and the hydrogel networks become too compact and unable to sustain deformation. In addition, for Na-alginate/PNIPAM hydrogel

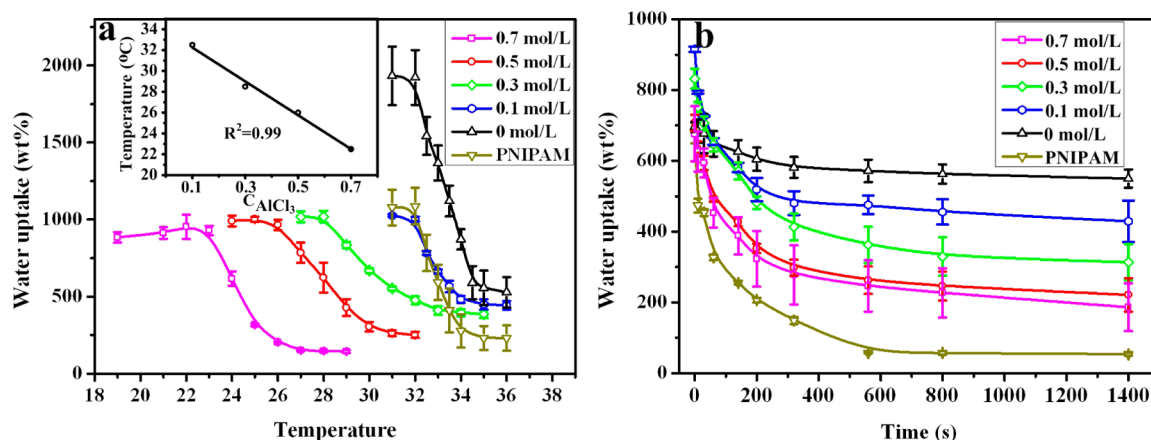


Figure 4. Thermoresponsive properties of the Al-alginate/PNIPAM hydrogel. (a) Water uptake of Al-alginate/PNIPAM (0.03, γ) hydrogels and pure PNIPAM hydrogel at various temperatures; inset: LCST versus the AlCl_3 concentration, the correlation coefficient is 0.99. (b) Deswelling kinetics for Al-alginate/PNIPAM (0.03, γ) and pure PNIPAM hydrogels when the hydrogels were transferred from water bath at 20 to 45 °C. γ is the Al^{3+} concentration, $\gamma = 0, 0.1, 0.3, 0.5, 0.7$ mol/L. $\gamma = 0$ represents the Na-alginate/PNIPAm hydrogel.

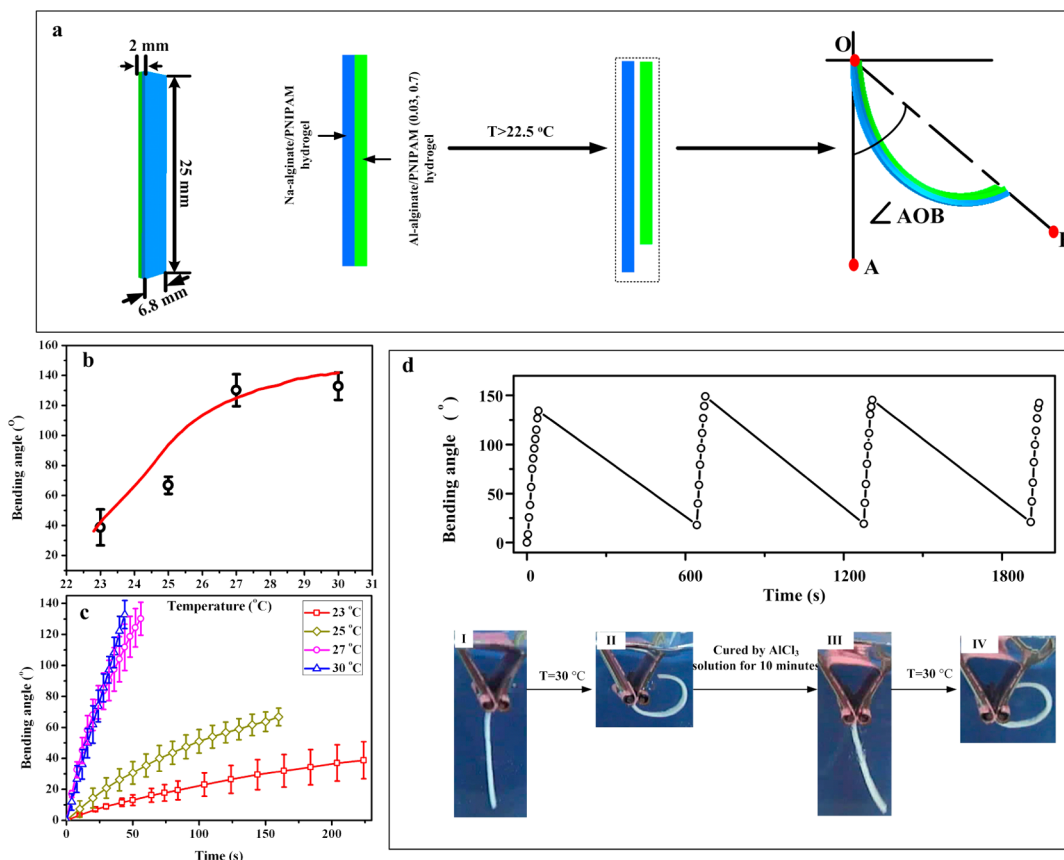


Figure 5. Actuation of (Na-alginate/PNIPAM)/(Al-alginate/PNIPAM) bilayer hydrogel actuator. (a) Sketch of a bilayer beam actuator and the definition of bending angle. At temperature above LCST of Al-alginate/PNIPAM, 22.5 °C in this case, the composite beam bends toward Al-alginate/PNIPAM hydrogel due to the anisotropic deswelling of the bilayer, defining the bending angle as $\angle \text{AOB}$. (b) Bending angle of the bilayer beam actuator at different temperatures; the red line represents the prediction, and the dots represent experimental data. (c) Change in bending angle in response to time at different temperatures. (d) Reversible bending behavior of the actuator when it was put into and then pulled out of 30 °C water. For each cycle, when the extreme of bending angle, 140°, was reached after 40 s, the bilayer was cured in a 0.7 mol/L AlCl_3 solution for 10 min, and it gradually recovered to its original undeformed position.

and pure PNIPAM hydrogels, the measured strength is only 15.3 ± 0.6 and 18.1 ± 0.7 kPa, and the Young's modulus is 1.4 ± 0.9 and 2.3 ± 0.1 kPa, respectively.

Besides, the concentration of Al^{3+} also affects the tensile stress of the tough Al-alginate/PNIPAM hydrogel. Figure 2b presents

the tensile test results of Al-alginate/PNIPAM (0.03, γ) hydrogels, where γ is the molar concentration of Al^{3+} ions ($\gamma = 0.1, 0.3, 0.5, 0.7$ mol/L), and MBAA concentration is 0.03 mol %. The increase of Al^{3+} concentration results in increase of uniaxial stretch (the maximum is ~ 10) but decrease of tensile stress. This

trend may be explained as follows. When PNIPAM polymers dissolve in water, a high ordered hydration shell formed, due to the hydrogen bonds between water and the amide groups. The salts in solution can polarize the water molecular and promote the collapse of the hydration shell, resulting in the exposure of the hydrophobic groups of PNIPAM polymers. Thus, the exposed hydrophobic groups aggregate with each other owing to the entropy gain,²⁵ which leads to the polymer chains curling in salt solution, and the polymer chains change from tight to the loose status. The loose polymer chains in the hydrogel networks result in high uniaxial stretch but low tensile stress.

Also note that in tensile test of tough Al-alginate/PNIPAM hydrogels, a distinct yield point is observed in the stress–stretch curves at ~ 2.5 of stretch (Figure 2a, b). Images of the yield phenomena of the hydrogel deformed at different stretches are shown in Figure 2c. After the yield point, hydrogel deformation became inhomogeneous and necked region and un-necked region coexisted. The necked region deformed more than the un-necked region under tensile stress, resulting in the thinner body of the necked region which broke at last. The yielding phenomenon is one of the characteristic features of tough hydrogels.^{23,26} The yielding behavior of the Al-alginate/PNIPAM hydrogel may correspond to unzip the networks of ionic cross-linked alginate.

The tough hydrogel can exhibit even superior properties in compression (Figure 3). Al-alginate/PNIPAM (0.03, 0.3) hydrogel can sustain a 6.3 ± 0.3 MPa of compressive stress when compressed at 95%, which is ~ 10 times that of the pure PNIPAM hydrogel (0.65 ± 0.2 MPa). At large compression strain of 80%, the tough hydrogel can dissipate energy 1610 ± 30.9 kJ/m³ in one complete cycle (Figure 3b) and demonstrate excellent recovery after compression (Figure 3c).

The tough Al-alginate/PNIPAM outperforms overwhelmingly as compared with pure PNIPAM hydrogel and Na-alginate/PNIPAM hydrogel, showing substantial increase in tensile and compressive strength, Young's modulus, energy dissipation, and recoverability. The physical and chemical mechanism of enhancement of tough hydrogels can be understood as follows. The Al³⁺ cations cross-link alginate via electrostatic interaction with carboxylic groups (COO⁻) on alginate polymer chains. The physical cross-linking between Al³⁺ cations and alginate is reversible. Decross-linking ionic bonding dissipates energy under large deformation; coexisting of both chemical and physical cross-links and interpenetrating of long-chain PNIPAM networks increase elasticity of hydrogels, which contributes to recovery of its original configuration after deformation. The synergy of these two mechanisms enhances the mechanical performance of Al-alginate/PNIPAM.^{23,27}

The effects of AlCl₃ are twofold: strengthening alginate/PNIPAM and tuning the LCST of Al-alginate/PNIPAM hydrogels. As shown in Figure 4, increasing AlCl₃ concentration in the range of 0.1–0.7 mol/L linearly decreases LCST of the hydrogels from 32 to 22.5 °C, which is analogous to the so-called Hofmeister effects of salt on LCST of PNIPAM.²⁶ Deswelling kinetics experiments (Figure 4b) illustrate that Al-alginate/PNIPAM hydrogel also bears the feature of rapid response and large volume shrinkage: the deswelling equilibrium time reduces from ~ 600 s of PNIPAM hydrogels to ~ 300 s of tough hydrogel; equilibrium water loss increases from ~ 350 wt % of Na-alginate/PNIPAM hydrogel to ~ 650 wt % of Al-alginate/PNIPAM (0.03, 0.7) hydrogel. The prevailing mobile Al³⁺ cations generate higher osmotic pressure between inside and outside of hydrogel; cross-linking of alginate by Al³⁺ cations also reduces hydrophilicity of

Al-alginate/PNIPAM as compared to Na-alginate/PNIPAM hydrogel.

Based on the different LCST values of those hydrogels, it is possible to design a bilayer construction hydrogel actuator. We fabricate a bilayer (Na-alginate/PNIPAM)/(Al-alginate/PNIPAM (0.03, 0.7)) hydrogel beam with the size of 25 mm \times 6.8 mm \times 2 mm as schematized in Figure 5a. Due to different LCST values of the two layers of this composite beam, immersing the beam into a water bath at temperature above 22.5 °C will cause the bending of the beam toward Al-alginate/PNIPAM hydrogel, and a bending angle $\angle AOB$ is measured.

We model the actuation process of bilayer (Na-alginate/PNIPAM)/(Al-alginate/PNIPAM (0.03, 0.7) hydrogel beam by using the commercial software, ABAQUS SIMULIA 6.10. The core of our methodology is to construct the free energy density of the hydrogel composites.²⁸ Adopting the Flory–Huggins model, the free energy per reference volume of the temperature-sensitive hydrogel is expressed as

$$W(I_1, I_3, T) = \frac{1}{2} N k_B T (I_1 - 3 - 2 \log I_3) + \frac{k_B T}{\nu} I_3 [(1 - \phi) \ln(1 - \phi) + \chi \phi (1 - \phi)] \quad (3)$$

where $I_1 = F_{ik} F_{ik}$ and $I_3 = \det \mathbf{F}$ are the first and the third invariants of the deformation gradient tensor, T is temperature, ϕ is the volume fraction of polymer and related to I_3 via $I_3 = 1/\phi$, N is the number of chains per polymer volume, ν is the volume of a solvent molecule, and k_B is the Boltzmann constant. Equation 3 has two sources: the elastic energy due to stretching of the network which is assumed to be isotropic and approximated by the neo-Hookean model, and the mixing energy of polymer and solvent. The hyperelastic model used herein assumes isotropic properties but allows large deformation.

The Flory–Huggins interaction parameter, χ , measures the enthalpy of mixing process and is expressed in terms of T and ϕ for a temperature-sensitive hydrogel

$$\chi(T, \phi) = A_0 + B_0 T + (A_1 + B_1 T) \phi \quad (4)$$

The coefficients, A_i and B_i , are fitted to LCST measurements of various hydrogels. For the Al-alginate/PNIPAM (0.03, 0.7) hydrogel, the four coefficients, A_0 , B_0 , A_1 , and B_1 , are $A_0 = -12$, $B_0 = 0.0423$, $A_1 = 17$, and $B_1 = -0.0567$; coefficients for Na-alginate/PNIPAM hydrogel are $A_0 = -14.12$, $B_0 = 0.0483$, $A_1 = 17.44$, and $B_1 = -0.0557$. Dimensionless parameter $N\nu$ used in simulation for these two types of hydrogels is 0.01 and 0.0037, respectively.

Figure 5b shows the maximum bending angle of the bilayer beam at different temperatures. The experimental results (dots) fit the simulation results (line) very well. The bending angle increases with the temperature until 27 °C and then keeps constant. It is because the deswelling of Al-alginate/PNIPAM (0.03, 0.7) happens in the temperature range of 22.5–27 °C (Figure 4a), and the shrinking of this layer stops after 27 °C and the bending angle keeps constant. The actuation kinetics of the beam actuator at different temperature is shown in Figure 5c. The bending angle and speed can be controlled by tuning the temperature. A maximum bending angle of $\sim 140^\circ$ was obtained when temperature > 27 °C and bending process finished within 50 s. The bending of the actuator is also reversible, and Figure 5d shows the cyclic bending process when the actuator was put into and then pulled out of the hot water bath.

The numerical simulation methodology helps us to understand and regulate the deformation of more complex all-hydrogel

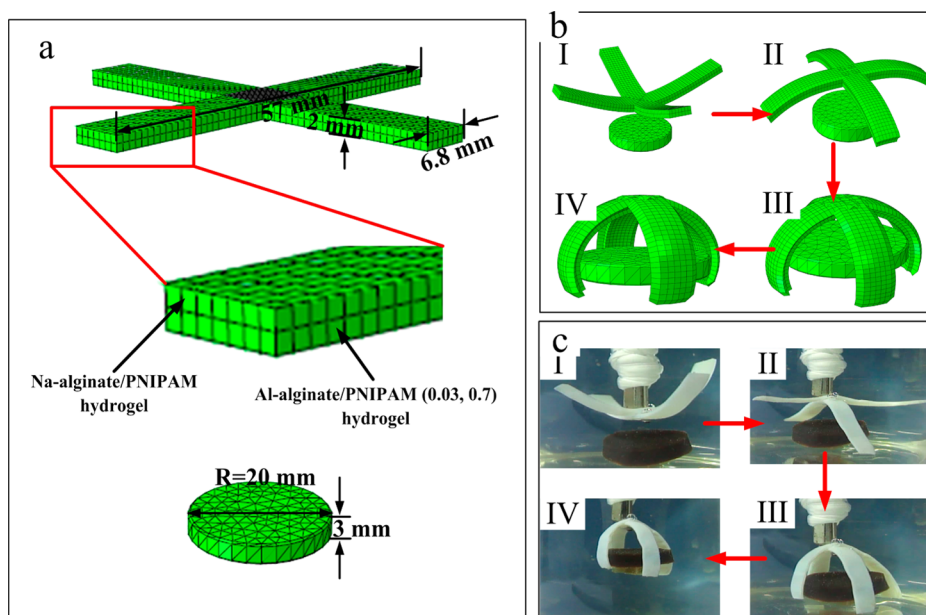


Figure 6. Snapshots of experiment and FE simulation of gripping of a hydrogel disc by a four-arm gripper. (a) Dimensions and FE mesh of the gripper and the hydrogel disc. Each arm of the gripper is made of a bilayer strip, with Na-alginate/PNIPAM hydrogel being the upper layer and Al-alginate/PNIPAM (0.03, 0.7) being the lower layer. (b) Snapshots of the FE simulation of the gripping process. The initial bending curvature of the gripper is mimicked by applying an upward buoyance pressure. Contacts between the gripper and the object were well-defined. (c) Images of the gripping process of the four-arm gripper captured a black hydrogel disc. When immersing the gripper into a 45 °C water bath, the original transparent Al-alginate/PNIPAM gripper bends upward due to buoyance and becomes opaque instantaneously.

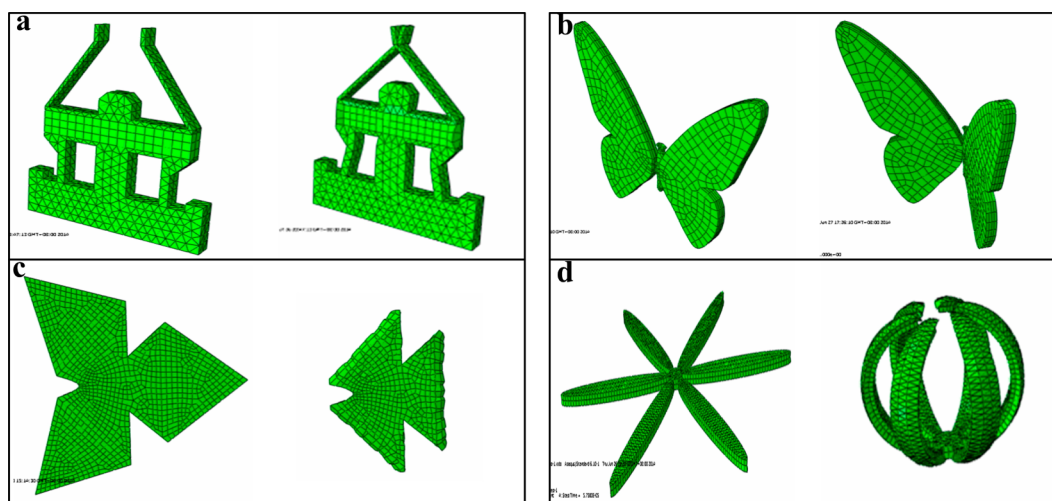


Figure 7. Predicted deformation of other possible soft robotic designs: (a) microgripper; (b) butterfly shape; (c) triangular shape; (d) star shape.

structures. Understanding the working principle of actuator,¹⁰ we design a four-arm gripper as a demonstration of prototype soft robotics (Figure 6a), carry out FE simulation (Figure 6b), and validate the simulation by experiment (Figure 6c). Due to the friction between the gripper arm and the hydrogel disc (the friction coefficient used in our simulation is taken from the literature of friction test of gel/gel²⁹ and fixed to 0.1), lifting the gripper also elevates the weight (a black hydrogel disc). The initial upward bending of the gripper, the friction and contact between the gripper, and the object were well-defined. The simulation mimics the gripping process very well and also predicts ~200 Pa contact force. By adding the weight of the load gradually in the simulation, the predicted maximum loads that can be lifted by the gripper is ~1.21 g. Figure 6c shows the gripping process of a 0.52 g black hydrogel disc by the gripper.

Each arm of the gripper is made of a bilayer strip, with Na-alginate/PNIPAM hydrogel being the upper layer and Al-alginate/PNIPAM (0.03, 0.7) being the lower layer. When immersing the gripper into a 45 °C water bath, the original transparent Al-alginate/PNIPAM gripper bends upward due to buoyance and becomes opaque instantaneously. The anisotropic shrinkage of the hydrogels causes the arms to bend downward, contact the object, and exert normal pressure to the object.

Meanwhile, a series of intriguing self-folding and pattern formations are simulated by FE simulation in Figure 7 including microgripper (a), butterfly shape (b), triangular shape (c), and star shape (d). Those constructions are capable of performing the action of gripping, flapping, and curling driven by temperature changing.

4. CONCLUSION

In summary, we report synthesis of tough, temperature-sensitive Al-alginate/PNIPAM hydrogel with tunable LCST. Interpenetrating long-chain PNIPAM networks with chemical cross-linking and cross-linking alginate by Al³⁺ cations strengthen the resultant hybrid hydrogels. Varying the concentration of AlCl₃ can tune the LCST of the hydrogel within a range from 22.5 to 32 °C, enabling operation of the all-hydrogel actuators with bilayer (Na-alginate/PNIPAM)/(Al-alginate/PNIPAM) structure at room temperature. Enhancing mechanical properties and tuning LCST of hydrogels also pave the way for realization of soft robotics that can sustain loads, grip, and elevate a weight. A bending beam actuator and a four-arm gripper are demonstrated. We also develop a numerical simulation strategy to predict the actuation of those actuators and grippers, and excellent agreement is achieved between simulation and experiment. Extending such tough hydrogels with varying thermosensitivity and stiffness for other intriguing fields such as self-folding or pattern formation is expected.

AUTHOR INFORMATION

Corresponding Authors

*E-mail: chenym@mail.xjtu.edu.cn.

*E-mail: jxzhouxx@mail.xjtu.edu.cn.

Notes

The authors declare no competing financial interest.

ACKNOWLEDGMENTS

This research was supported by National Natural Science Foundation of China (Grants 51173144, 11372239, 51073127, 11472210, 11321062), the Research Fund for the Doctoral Program of Higher Education of China, Scientific Research Foundation for the Returned Overseas Chinese Scholars, State Education Ministry, the Fundamental Research Funds for the Central Universities, International Science & Technology Cooperation Program Supported by Ministry of Science and Technology of China and Shaanxi Province (2013KW14-02), and Key Innovational Research Team Program Supported by Shaanxi Province (2013KCT-05).

REFERENCES

- (1) Dong, L.; Jiang, H. R. pH-Adaptive Microlenses Using Pinned Liquid-Liquid Interfaces Actuated by pH-Responsive Hydrogel. *Appl. Phys. Lett.* **2006**, *89*, 211120.
- (2) Dong, L.; Agarwal, A. K.; Beebe, D. J.; Jiang, H. R. Adaptive Liquid Microlenses Activated by Stimuli-Responsive Hydrogels. *Nature* **2006**, *442*, 551–554.
- (3) Liu, Z. S.; Calvert, P. Multilayer Hydrogels as Muscle-Like Actuators. *Adv. Mater.* **2000**, *12*, 288–291.
- (4) Brochu, P.; Pei, Q. B. Advances in Dielectric Elastomers for Actuators and Artificial Muscles. *Macromol. Rapid Commun.* **2010**, *31*, 10–36.
- (5) Hamidi, M.; Azadi, A.; Rafiei, P. Hydrogel Nanoparticles in Drug Delivery. *Adv. Drug Delivery Rev.* **2008**, *60*, 1638–1649.
- (6) Qiu, Y.; Park, K. Environment-Sensitive Hydrogels for Drug Delivery. *Adv. Drug Delivery Rev.* **2001**, *53*, 321–339.
- (7) Seliktar, D. Designing Cell-Compatible Hydrogels for Biomedical Applications. *Science* **2012**, *336*, 1124–1128.
- (8) Stuart, M. A.; Huck, W. T.; Genzer, J.; Muller, M.; Ober, C.; Stamm, M.; Sukhorukov, G. B.; Szleifer, I.; Tsukruk, V. V.; Urban, M.; Winnik, F.; Zauscher, S.; Luzinov, I.; Minko, S. Emerging Applications of Stimuli-Responsive Polymer Materials. *Nat. Mater.* **2010**, *9*, 101–113.

- (9) Wang, E.; Desai, M. S.; Lee, S. W. Light-Controlled Graphene-Elastin Composite Hydrogel Actuators. *Nano Lett.* **2013**, *13*, 2826–2830.

- (10) Ilievski, F.; Mazzeo, A. D.; Shepherd, R. F.; Chen, X.; Whitesides, G. M. Soft Robotics for Chemists. *Angew. Chem., Int. Ed. Engl.* **2011**, *50*, 1890–1895.

- (11) Pelah, A.; Seemann, R.; Jovin, T. M. Reversible Cell Deformation by a Polymeric Actuator. *J. Am. Chem. Soc.* **2007**, *129*, 468–469.

- (12) Zhang, X.; Pint, C. L.; Lee, M. H.; Schubert, B. E.; Jamshidi, A.; Takei, K.; Ko, H.; Gillies, A.; Bardhan, R.; Urban, J. J.; Wu, M.; Fearing, R.; Javey, A. Optically- and Thermally-Responsive Programmable Materials Based on Carbon Nanotube-Hydrogel Polymer Composites. *Nano Lett.* **2011**, *11*, 3239–3244.

- (13) Guan, Y.; Zhang, Y. J. PNIPAM Microgels for Biomedical Applications: From Dispersed Particles to 3D Assemblies. *Soft Matter* **2011**, *7*, 6375–6384.

- (14) Zhang, X. Z.; Wu, D. Q.; Chu, C. C. Synthesis, Characterization, and Controlled Drug Release of Thermosensitive IPN-PNIPAAm Hydrogels. *Biomaterials* **2004**, *25*, 3793–3805.

- (15) Haraguchi, K.; Takehisa, T.; Fan, S. Effects of Clay Content on the Properties of Nanocomposite Hydrogels Composed of Poly(*N*-isopropylacrylamide) and Clay. *Macromolecules* **2002**, *35*, 10162–10171.

- (16) Fei, R. C.; George, J. T.; Park, J.; Means, A. K.; Grunlan, M. A. Ultra-Strong Thermoresponsive Double Network Hydrogels. *Soft Matter* **2013**, *9*, 2912–2919.

- (17) Haraguchi, K.; Li, H. J. Control of the Coil-to-Globule Transition and Ultrahigh Mechanical Properties of PNIPAAm in Nanocomposite Hydrogels. *Angew. Chem., Int. Ed. Engl.* **2005**, *44*, 6500–6504.

- (18) Xia, L. W.; Xie, R.; Ju, X. J.; Wang, W.; Chen, Q.; Chu, L. Y. Nano-Structured Smart Hydrogels with Rapid Response and High Elasticity. *Nat. Commun.* **2013**, *4*, 2226.

- (19) Guvendiren, M.; Yang, S.; Burdick, J. A. Swelling-Induced Surface Patterns in Hydrogels with Gradient Crosslinking Density. *Adv. Funct. Mater.* **2009**, *19*, 3038–3045.

- (20) Sharon, E. Swell Approaches for Changing Polymer Shapes. *Science* **2012**, *335*, 1179–1180.

- (21) Kim, J.; Hanna, J. A.; Byun, M.; Santangelo, C. D.; Hayward, R. C. Designing Responsive Buckled Surfaces by Halftone Gel Lithography. *Science* **2012**, *335*, 1201–1205.

- (22) Sun, J. Y.; Zhao, X.; Illeperuma, W. R.; Chaudhuri, O.; Oh, K. H.; Mooney, D. J.; Vlassak, J. J.; Suo, Z. Highly Stretchable and Tough Hydrogels. *Nature* **2012**, *489*, 133–136.

- (23) Yang, C. H.; Wang, M. X.; Haider, H.; Yang, J. H.; Sun, J. Y.; Chen, Y. M.; Zhou, J. X.; Suo, Z. Strengthening Alginate/Polyacrylamide Hydrogels Using Various Multivalent Cations. *ACS Appl. Mater. Interfaces* **2013**, *5*, 10418–10422.

- (24) Al-Musa, S.; Abu Fara, D.; Badwan, A. A. Evaluation of Parameters Involved in Preparation and Release of Drug Loaded in Cross-Linked Matrices of Alginate. *J. Controlled Release* **1999**, *57*, 223–232.

- (25) Zhang, Y.; Furry, S.; Bergbreiter, D. E.; Cremer, P. S. Specific Ion Effects on the Water Solubility of Macromolecules: PNIPAAm and the Hofmeister Series. *J. Am. Chem. Soc.* **2005**, *127*, 14505–14510.

- (26) Zhao, Y.; Nakajima, T.; Yang, J. J.; Kurokawa, T.; Liu, J.; Lu, J.; Mizumoto, S.; Sugahara, K.; Kitamura, N.; Yasuda, K.; Daniels, A. U.; Gong, J. P. Proteoglycans and Glycosaminoglycans Improve Toughness of Biocompatible Double Network Hydrogels. *Adv. Mater.* **2014**, *26*, 436–442.

- (27) Zhao, X. H. Multi-Scale Multi-Mechanism Design of Tough Hydrogels: Building Dissipation into Stretchy Networks. *Soft Matter* **2014**, *10*, 672–687.

- (28) Guo, W.; Li, M. E.; Zhou, J. X. Modeling Programmable Deformation of Self-Folding All-Polymer Structures with Temperature-Sensitive Hydrogels. *Smart Mater. Struct.* **2013**, *22*, 115028.

- (29) Kagata, G.; Gong, J. P. Surface Sliding Friction of Negatively Charged Polyelectrolyte Gels. *Colloids Surf., B* **2007**, *56*, 296–302.